Test Models for Stability/Security Studies of AC-DC Hybrid Power Systems with High Penetration of Renewables

Huadong Sun, *Senior Member, IEEE*, Bing Zhao, *Member, IEEE*, Shiyun Xu, *Member, IEEE*, Tiankai Lan, Zonghan Li, and Ping Wu

***Abstract*—Modern bulk power systems are developing into AC-DC hybrid systems with high penetration of renewables. There has been a lack of representative benchmarks to study stability and security problems of modern power systems. This paper presents an attempt to provide a set of four test models, addressing problems of voltage stability, rotor angle stability, frequency stability, and power frequency overvoltage under large disturbance. On the four stability/security problems, the models consider both their conventional features and distinct features induced by renewables. All the data of the models are extracted from real power systems, with modifications to establish a near-future scenario with over 50% renewable penetration. The test models are proposed by China Electric Power Research Institute, and acknowledged by Chinese Society for Electrical Engineering (CSEE). They are expected to serve educators, researchers and practitioners in related areas.**

***Index Terms*—Power system with renewables, AC-DC hybrid system, test model, benchmark**

I. Introduction

Modern power systems are developing into AC-DC hybrid systems with high penetration of renewables. Currently, HVDC is being widely applied for interregional transmission and offshore renewables integration. Renewables are expected to satisfy over 80% load energy demand by 2050 in the USA [1]. The percentage is expected to be 60% in China, and as much as 100% in several European countries [2]-[3].

Compared to conventional power systems, modern power systems are faced with new stability and security problems. Extensive researches have been carried out in related fields. This exposes the demand for benchmark test models. A well-established benchmark helps to relieve the researchers' effort in configuring and tuning their testbed, and makes it possible to compare various methods and schemes in one same environment.

In past decades, several existing benchmarks have played an important role in electric research and education, such as WECC-9 bus system [4], 4-machine-2-area system [5], IEEE-39 bus system [6], and IEEE-118 bus system [7]. However, these benchmarks are established years ago. Most of them do not contain any renewables or HVDCs. When using these benchmarks, people have to pay much effort to revise the system and specify renewable/HVDC parameters. Even with these efforts, it is still difficult to ensure rationality of the testbed. Besides, different literatures generally make different modifications on the models. It is difficult to make comparison between different literatures and algorithms. A testbed with inherent renewables/HVDCs can significantly help with the problem.

In addition, renewables are causing distinct stability and security problems in practical projects. These are hardly reflected in existing benchmarks. Low-voltage-ride-through (LVRT) of photovoltaics (PVs) and wind farms demonstrates complex performances in high-penetration scenarios. Hydro power contributes to ultra-low frequency oscillation, which is the crucial engineering problem in several areas around the world [8]-[9]. Wind farms are found to interact with HVDCs and causes severe overvoltage in HVDC sending-end systems [10]-[11]. Among the literatures, these phenomena are investigated in various power systems, with limited system data revealed. Comparative studies are hardly conducted. This again calls for benchmark test models of modern power systems.

In view of the above, China Electric Power Research Institute (CEPRI) has made an attempt to establish representative test models for stability/security study of modern power systems under large disturbance. The works are then acknowledged and recognized by Chinese Society for Electrical Engineering (CSEE). This paper presents a set of four electromechanical test models, respectively constrained by voltage stability, rotor angle stability, frequency stability, and power frequency overvoltage problems. Various operating scenarios are configured in each model, reflecting different aspects of the above problems. The models are with the following features, making up for deficiencies of existing benchmarks.

1) The test models are AC-DC hybrid systems with over 50% renewable penetration, emphasizing on the challenging operating scenario in near future.
2) The test models reflect both conventional stability/security features and new distinct features induced by renewables.
3) All the models are extracted from real engineering projects. Practical considerations such as electrical

This work was supported by National Natural Science Foundation of China U21666601.

All the authors are with China National Key Laboratory of Power Grid Security (China Electric Power Research Institute).

distance and distribution of renewables are inherently considered for the convenience of users.

The rest of this paper is organized as follows. Section II describes main features of the established models, including phenomenon and mechanism of the considered stability/security problems, as well as authenticity of model data. Section III gives descriptions of all the four test models, along with simulation validations. Section IV further test performance of the models for various influencing factors, for reference of any users. Conclusions are given in Section V. Further details of the models are enclosed in the Supplementary Documents of this paper, and can be found at https://github.com/lbl-hub/CSEE.

II. Main Features of the Models

The established models emphasize on major constraint stability/security problems in real engineering scenarios with over 50% renewable penetration. Several new, renewable-induced distinct features are also incorporated. All the models and features are extracted from real power systems, and are established in electromechanical timescale.

A. Consideration of Stability/Security Problems under Large Disturbance

All the models and scenarios are summarized in TABLE I, along with the related stability/security problems. Every one of the models is extracted from a real power system, addressing one of the stability/security problems. On this basis, two or three operating scenarios are configured in each model, reflecting various aspects and phenomena of the problem. Several new, distinct features induced by renewables are incorporated in the models as well.

1) **Voltage Stability and Model CSEE-VS**

Voltage stability in this paper refers to short-term voltage stability, whose definition is given in [15]. In simulations, two kinds of phenomenon are regarded as voltage instability, i.e., voltage collapse and continuous low voltage.

Voltage collapse means the post-fault voltage drops to a very low level, and do not recover again. Continuous low voltage is similar to the so-called fault-induced delayed voltage recovery, in which the voltage recovers very slowly or keeps in a relatively low level (e.g., 0.8p.u.) [16]-[17].

Renewable LVRT participates in voltage dynamics in high penetration scenarios, and creates distinct features. When the voltage is operating around LVRT threshold (usually 0.85p.u.~0.95p.u.), renewables get in and out of LVRT control repeatedly. This in turn stimulates voltage oscillation. Such phenomenon is reported in several wind farms in Northwest China and incorporated in the benchmark.

In addition, with decrease of synchronous generators, reactive power sources of the system also decrease. This requires more shunt capacitors and synchronous condensers. Transient voltage performance of the system is therefore different form conventional power systems.

In view of the above new features, a model named CSEE-VS is established for voltage stability study. The model is with two operating scenarios, respectively addressing voltage collapse and continuous low voltage. The LVRT-induced distinct features are reflected in both scenarios.

Post-fault low voltage occasionally leads to instabilities other than voltage instability, such as rotor angle instability and high frequency. Besides, continuous low voltage in practical system would trigger load disconnection or other events, which is not modelled in short-term simulations.

2) **Rotor Angle Stability and Model CSEE-RAS**

There are two kinds of rotor angle stability (RAS) followed by a large disturbance, i.e., transient RAS (aperiodic RAS) and dynamic RAS (periodic RAS) [18]-[19]. In transient RAS, system lose synchronism in the first or second swing. In dynamic RAS, the rotor angle keeps oscillating at a certain frequency. Features of the stabilities can be varied with varied renewable penetration [20]. Notably, dynamic RAS is different from small-disturbance oscillatory stability in IEEE definition [15], as it follows a large disturbance.

A model named CSEE-RAS is established for rotor angle stability study. The model is with two operating scenarios, respectively addressing transient RAS and dynamic RAS. In further test of the model (Section IV), effect of renewables are

TABLE I
Overview of All the Models and Scenarios

Stability/Security Problem (names of the models)	Basic Real Power System	Related Phenomenon (designed scenarios of the models)	Distinct Renewable-Induced Features
Voltage Stability (model CSEE-VS)	Qishao HVDC Receiving-End System	Voltage Collapse	LVRT-Induced Voltage Oscillation [12], [13]
		Continuous Low Voltage	
Rotor Angle Stability (model CSEE -RAS)	Part of China Southern Power Grid (Guizhou, Guangxi, and Guangdong)	Dynamic (Periodic) RAS	Influence on Damping Ratio and Critical Clearing Time
		Transient (Aperiodic) RAS	
Frequency Stability (model CSEE -FS)	Part of China Southwest Power Grid (Sichuan, Chongqing and Xizang/Tibet)	Low Frequency	Hydro-Power-Induced Ultra-Low Frequency Oscillation
		High Frequency	
		Ultra-Low Frequency Oscillation	
Power Frequency Overvoltage (model CSEE -PFO)	Jiquan HVDC Sending-End System	Temporary PFO	Renewable Participated/ Constrained PFO and PFO induced by HVDC block-out [14]
		Continuous PFO	

observed in several quantifying indices, such as damping ratio and critical clearing time (CCT).

3) **Frequency Stability and Model CSEE-FS**

Frequency stability is becoming more prominent in modern power systems, as most renewables and HVDCs offer little inertial and frequency support [21]. Besides, HVDC fault results more significant power imbalance than any synchronous generators, and deteriorates frequency stability of the system.

In practical engineering, conventional frequency stability is treated more likely a security problem, rather than stability problem. From the perspective of dynamics theory, the system can operate stably with a very high or low frequency. However, an abnormal frequency can trigger unexpected control actions, and is harmful to electric components like rotating machines.

Notably, there is a distinct frequency stability phenomenon rooting from dynamic response of hydraulic turbine, that is ultra-low frequency oscillation. The phenomenon has been reported in several power systems around the world [8]-[9]. Frequency of the overall system oscillates at 0.01Hz~0.1Hz, resulting from water hammer effect of hydro power plant.

A model named CSEE-FS is established for frequency stability study. The model is with three operating scenarios, respectively addressing high frequency, low frequency, and ultra-low frequency oscillation in modern power systems.

4) **Power Frequency Overvoltage and Model CSEE-PFO**

Overvoltage is becoming an important issue in modern power systems, as most renewable energy sources are interfaced with power electronic devices. They are sensitive to overvoltage, and hardly help with voltage regulation.

In electromechanical timescale, power frequency overvoltage is one of the major security constraints in HVDC sending end system, especially when there exists a high penetration of renewables [10]-[11]. After AC fault or HVDC fault, surplus reactive power can easily lead to overvoltage, and further result in renewable disconnection. Notably, HVDC block-out decreases reactive power demand in the sending end, occasionally resulting in severe overvoltage.

A model named CSEE-PFO is established for power frequency overvoltage study. The model is with two operating scenarios, addressing temporary PFO and continuous PFO respectively, and covers the PFO definitions in IEEE standard [22].

B. Considerations of Authenticity and Representativeness

To ensure authenticity of the test systems, CEPRI selects from real power systems that have been studied by the power system community in Asia. All the stability/security problems are real problems that have happened in the system or have been observed in simulation study. Dynamic elements such as HVDCs, renewables, and exciters are modelled from real elements in the power systems, with parameters only slightly modified to protect commercial sensitivities. The HVDCs are line-commutated HVDCs, renewables includes PVs, type-III winds, and type-IV winds. Load models in the test systems are similar to the composite model, with consideration of static load and motor. One may use some more advanced models to account for distributed energy resources [23]. The original real power systems of all the test systems have been given in TABLE I.

One other important feature is the modelling of renewable plants and converter stations. Dynamics inside renewable power plants have been widely recognized to affect renewable transient response, including but not limited to LVRT and overvoltage problems [24]-[25]. Therefore, the proposed models incorporate several power plants with relatively detailed topology. Topology of the plants are generally similar, regardless of PV or wind. Details of compensations, lines, and number of renewable sources may be varied in different scenarios. An example wind plant model is shown in Fig. 1, and an example PV plant model is shown in Appendix A. Such model helps to study the system with a better consideration of renewables and HVDCs, which is fairly important in modern power systems. Details of necessity of such renewable plant model can be found in simulation results in Section II. A and Section II. D (for LVRT and PFO study, respectively), which mainly lies in the consideration of terminal voltage of devices.

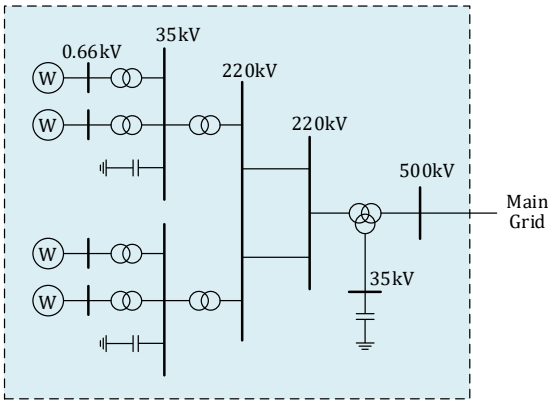

Fig. 1. An example of renewable plant model.

One other important issue is the scale and complexity of the test systems. Some very detailed, generic test systems are developed in the authors' previous works, containing various stability problems in one single case. However, it is found out to be very complex and more suitable for AI-based research, rather than mechanism analysis. Therefore, the test systems in this paper are proposed. Each system is focused on one stability/security issue, providing a straightforward (rather than coupled) testbed for research and education. Scale of the system approximate existing classical test systems, as they are larger than IEEE-39 and smaller than IEEE-118.

III. Descriptions and Validations of the Models

This section describes structure of all the four test models, along with their simulation results. Data of the models are given in Supplementary Document of this paper.

A. Voltage Stability Model CSEE-VS

Model CSEE-VS is an HVDC-receiving system, which is

extracted from the receiving end of Qishao HVDC, Hunan Province, China. The test model is comprised of 4 thermal power plants, 2 wind farms, and 1 PV plant. In some of the operating scenarios, synchronous condensers are applied as well. The main grid is with 20 nodes of 500kV, as demonstrated in Fig. 2. The model also includes 46 nodes of lower voltage level, depicting details of power plants, converter stations, and AC loads. These are not drawn in Fig. 2, but enclosed in the Supplementary Document of this paper.

Two operating scenarios are established, reflecting post-fault voltage collapse and post-fault continuous low voltage phenomenon. Several distinct renewable-induced features can be found in the benchmark. They will be addressed in Section IV and Supplementary Document of this paper.

1) **Scenario: Post-Fault Voltage Collapse**

In this scenario, generations and HVDC power level are summarized in TABLE II. Renewables take up 53.7% of overall generations. The constraint fault of this scenarios is a three-phase-to-ground fault of the line between bus_05 and bus_03, followed by an "N-2" line disconnection. After the N-2 fault, voltage of all buses in the system are in fairly low level. This leads to HVDC block-out and renewable disconnection. Voltage dynamics of the system is demonstrated in Fig. 3.

2) **Scenario: Post-Fault Continuous Low Voltage**

In this scenario, configuration of the system is kept the same as the former one, while two synchronous condensers are connected to bus_05. Each condenser is with the capacity of 300MVA.

The post-fault voltage response is demonstrated in Fig. 4. Notably, some special renewable-induced performances are observed, and will be addressed later in Section IV.

B. Rotor Angle Stability Model CSEE-RAS

Model CSEE-RAS is an HVDC-embedded system, which is extracted from three interconnected provincial grid of China (Guizhou, Guangxi, and Guangdong Province). The test model is with two areas, comprised of 7 thermal power plants, 3 wind farms, 5 PV plant, and 3 synchronous condensers. The main grid is with 11 nodes of 500kV, as demonstrated in Fig. 5. The model also includes 68 nodes with lower voltage level, depicting details of power plants, converter stations, and AC loads. The system can be roughly divided into a sending area and a receiving area, and synchronous generators are divided into two groups accordingly. In most occasions, rotor angle stability occurs between these two groups.

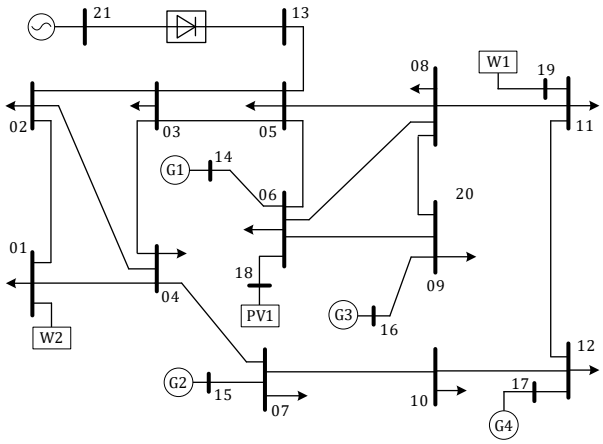

Fig. 2. Topology of CSEE-VS main grid.

TABLE II
POWER LEVEL OF GENERATIONS AND HVDC

	Thermal Plant				Wind Farm		PV	HVDC
Plant No.	G1	G2	G3	G4	W1	W2	PV1	/
Power Output (MW)	453	400	300	400	600	600	600	1600

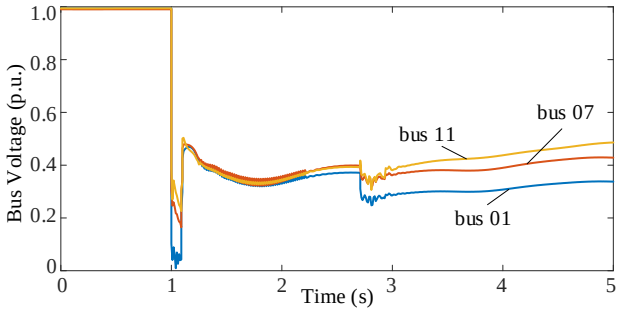

Fig. 3. Post-fault voltage collapse.

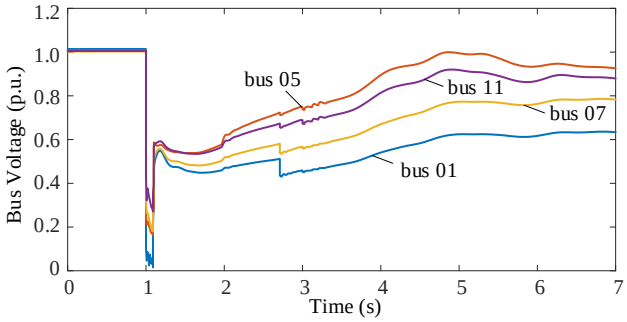

Fig. 4. Post-fault continuous low voltage.

Two operating scenarios are established for CSEE-RAS, reflecting post-fault dynamic (periodic) RAS and post-fault transient (aperiodic) RAS.

1) **Scenario: Post-Fault Dynamic (Periodic) RAS**

In this scenario, generations and HVDC power level are summarized in TABLE III. Renewables take up 50.3% of overall generations. The constraint fault of this scenarios is a three-phase-to-ground fault of the line between bus_01 and bus_11. The transmission line is then cut 0.1s later. Dynamic (periodic) rotor angle oscillation occurs after the fault.

The post-fault rotor angle dynamics are demonstrated in Fig. 6, with thermal plant G1 as reference. The lowest damping ratio in the system is 0.0039.

2) **Scenario: Post-Fault Transient (Aperiodic) RAS**

In this scenario, generations and HVDC power level are summarized in TABLE IV, with renewables taking up 50.1% overall generations. The constraint fault of this scenarios is kept as three-phase-to-ground fault of the line between bus_01 and bus_11. Transient (aperiodic) rotor angle instability occurs after the fault.

A timely fault-clearance can successfully prevent the instability. Critical clearing time (CCT) of this scenario is 0.156s. Figure 10 demonstrates rotor angle of the system with

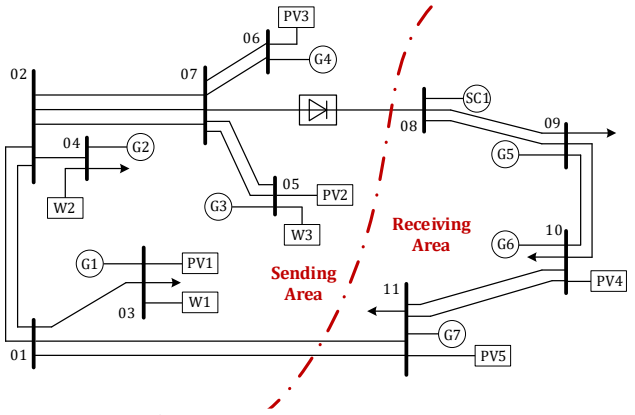

Fig. 5. Topology of CSEE-RAS main grid.

TABLE III
POWER LEVEL OF GENERATIONS AND HVDC

	Sending Area		Receiving Area		HVDC
	Thermal	Renewable	Thermal	Renewable	/
Power Level (MW)	1193	2300	1080	0	800

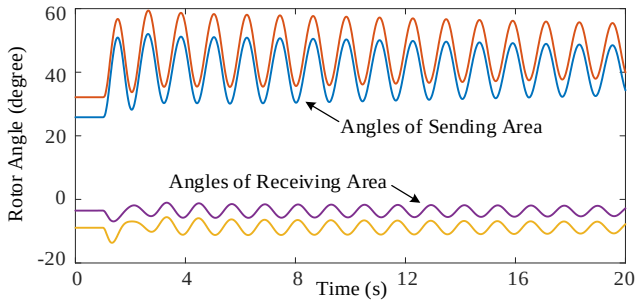

Fig. 6. Post-fault rotor angle oscillation.

a clearing time of 0.16s. The system lose stability.

C. Frequency Stability Model CSEE-FS

Model CSEE-FS is an HVDC sending-end system, extracted from Southwest Power Grid of China (covering Sichuan, Chongqing and Tibet). The test model is comprised of 3 HVDCs, 7 synchronous power plants (either thermal or hydro), 3 wind farms, and 2 PV plants. The main grid is with 16 nodes of 500kV, as demonstrated in Fig. 8. The model also includes 31 nodes of lower voltage level, depicting details of power plants, converter stations, and AC loads.

Three operating scenarios are established for CSEE-FS, respectively reflecting high frequency, low frequency, and ultra-low frequency oscillation. Notably, the ultra-low frequency oscillation is a distinct phenomenon that happens in several real power systems with high percentage of hydro power.

1) **Scenario: Post-Fault High Frequency**

In this scenario, generations and HVDC power level are summarized in TABLE V. PVs and wind farms take up 52.3% of overall generations. The typical fault of this scenario is HVDC-1 block out. The post-fault frequency response is demonstrated in Fig. 9. Three various HVDC power are configured in Fig. 9, for a better observation of frequency dynamics. Frequency stability of the system is evaluated through including frequency zenith, time of frequency zenith, and steady frequency deviation [26]. Value of all the indices are given in Table VI.

TABLE IV
POWER LEVEL OF GENERATIONS AND HVDC

	Sending Area		Receiving Area		HVDC
	Thermal	Renewable	Thermal	Renewable	/
Power Level (MW)	3273	3890	2100	1500	3000

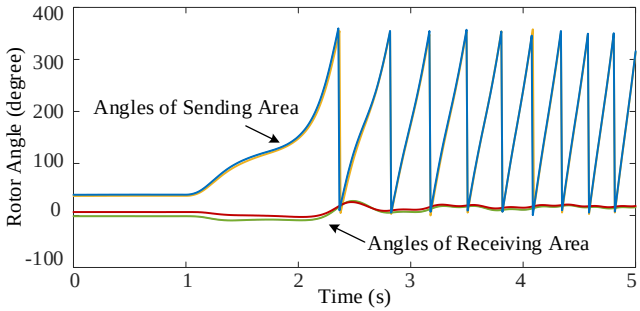

Fig. 7. Rotor angle dynamics with a fault clearing time of 0.16s.

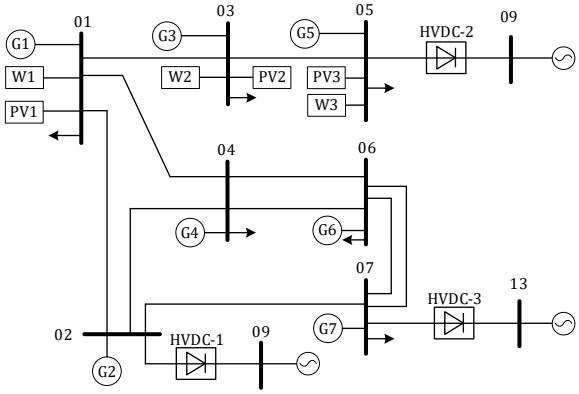

Fig. 8. Topology of CSEE-FS main grid.

TABLE V
POWER LEVEL OF GENERATIONS AND HVDC

	Thermal	Hydro	Wind	PV	HVDC
Power Level (MW)	2078	1400	1720	2090	2381

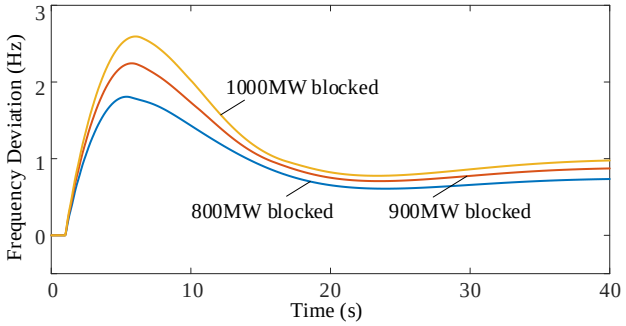

Fig. 9. Frequency dynamics after HVDC block-out.

2) **Scenario: Post-Fault Low Frequency**

In this scenario, generations and HVDC power level are all the same as the former scenario, as demonstrated in Table V. The typical fault is a generator disconnection. The post-fault frequency dynamics with various disconnected power are demonstrated in Fig. 10, with related evaluating indices listed in TABLE VII. Notably, the type of lost generator significantly affects system dynamics, as synchronous generators generally have better frequency regulation capability than renewable generators. The lost generators here are all synchronous ones. Impact of renewable generator lost are simulated and discussed in the Supplementary Document of the paper.

3) **Scenario: Post-Fault Ultra-Low Frequency Oscillation**

In this scenario, all the thermal power plants are replaced by hydro plants for a more typical ultra-low frequency oscillation phenomenon. The typical fault is configured as a three-phase-to-ground fault of line B03-B05, followed by an N-1 line disconnection.

Frequency dynamics of all the generators are demonstrated in Fig. 11. Frequency of all the generators oscillate in a coherent way, in ultra-low frequency.

D. Power Frequency Overvoltage Model CSEE-PFO

Model CSEE-PFO is an HVDC-sending system, which is extracted from Jiquan HVDC sending end, Xinjiang, China. The test model is comprised of 2 thermal plants, 4 wind farms, 2 PV farms and 2 synchronous condensers. The main grid is with 10 nodes of 500kV, as demonstrated in Fig. 12. The model also includes 58 nodes of lower voltage level, depicting details of connection of all power devices.

Two operating scenarios are established in CSEE-PFO, reflecting post-fault temporary PFO and post-fault continuous PFO.

1) **Scenario: Post-Fault Temporary PFO**

In this scenario, generations and HVDC power level are summarized in TABLE VIII. Renewables take up 58.1% of all generations. The typical fault of this scenarios is set as continuous commutation failure of HVDC, followed by an HVDC block-out.

Voltage dynamics of the point of common coupling (PCC) of HVDC are demonstrated in Fig. 13, together with voltage of PCC of wind farm W1. The maximum voltage are 1.38p.u. and 1.37p.u., respectively. This would trigger high-voltage disconnection of wind turbines.

Notably, analysis of PFO requires the detailed model of renewable plants, which is introduced in Fig. 1. This is because disconnections of renewables are dependent on terminal voltage of devices, which can be very different from the terminal of renewable plants.

2) **Scenario: Post-Fault Continuous PFO**

In this scenario, generations and HVDC power level are summarized in TABLE IX, with renewables taking up 50.5% overall generations. The typical fault of this scenarios is set as an HVDC block-out.

Voltage dynamics of PCC of HVDC are demonstrated in Fig. 14. In this scenario, the transient voltage does not exceed

TABLE VI
FREQUENCY STABILITY EVALUATION FOR FIG. 9

Blocked HVDC Power (MW)	Frequency Zenith (Hz)	Time of Frequency Zenith (s)	Steady Frequency Deviation (Hz)
800	1.83	5.99	0.74
900	2.22	6.34	0.87
1000	2.61	6.67	0.98

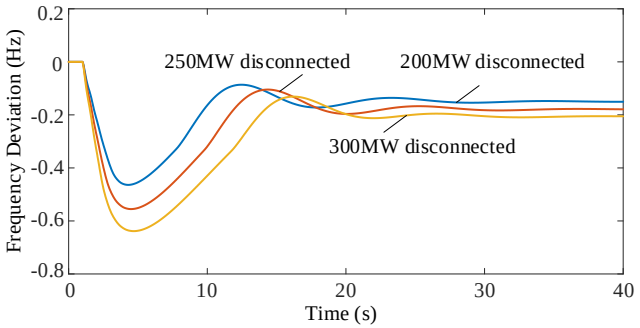

Fig. 10. Frequency dynamics after generator disconnection.

TABLE VII
FREQUENCY STABILITY EVALUATION FOR FIG. 10

Disconnected Power (MW)	Frequency Nadir (Hz)	Time of Frequency Nadir (s)	Steady Frequency Deviation (Hz)
200	-0.46	4.28	-0.15
250	-0.56	4.56	-0.18
300	-0.64	4.79	-0.21

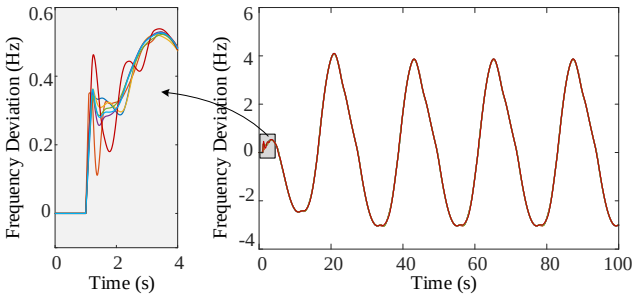

Fig. 11. Post-fault ultra-low frequency oscillation.

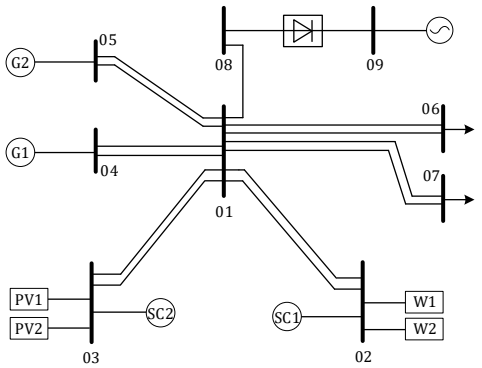

Fig. 12. Topology of CSEE-PFO main grid.

1.3p.u., which means renewable disconnection are not triggered. However, the post-fault voltage stays above 1.05p.u. continuously even all the compensations and filters are already disconnected. This is unacceptable for power system insulation in some areas, and threatens power system security.

TABLE VIII
POWER LEVEL OF GENERATIONS AND HVDC

	Thermal	Wind	PV	HVDC
Power Level (MW)	4620	3200	3200	1700

TABLE IX
POWER LEVEL OF GENERATIONS AND HVDC

	Thermal	Wind	PV	HVDC
Power Level (MW)	2750	1600	1200	3700

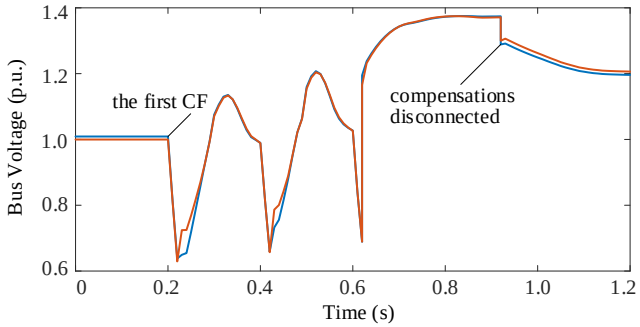

Fig. 13. Voltage dynamics of PCC of HVDC and wind farm W1.

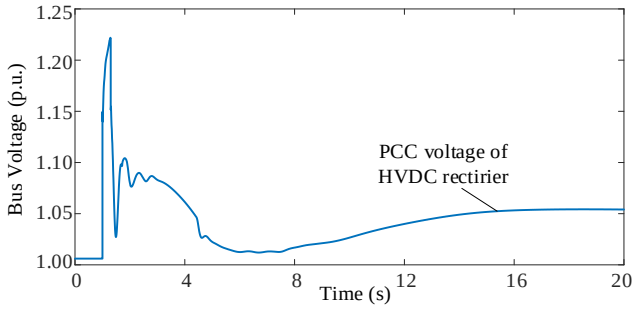

Fig. 14. Voltage dynamics of PCC of HVDC in continuous PFO scenario.

IV. FURTHER TEST OF THE MODELS

This section demonstrates further test of all the models in varied operating conditions. A number of influencing factors are considered and tested in 27 additional scenarios. In the tests, the four stability/security problems are intuitively evaluated through system performances. The stability/security problems and influencing factors are summarized in TABLE X. Details of the results are demonstrated partly in the main body of this paper, and partly in the Supplementary Document. The results can serve as a reference for users of the test models. Any user may further revise the model according to the demand.

A. Test of Voltage Stability Model CSEE-VS

In CSEE-VS, the voltage collapse scenario is tested with a number of varied influencing factors, including HVDC power level, renewable power level, configuration of condensers, and power load. Some of the tests are described as examples in the followings, and the rest are incorporated in the Supplementary Document.

Figure 15-16 demonstrate test results with varied HVDC power. With the decrease of HVDC power, stability of HVDC is enhanced, as well as the AC voltage. Figure 15 gives response of HVDC power in the voltage collapse scenario. Figure 16 gives voltage response of bus_05 in the continuous low voltage scenario.

Figure 17-18 demonstrate test results with varied renewable power. Figure 17(a)-(b) gives voltage response of different buses in the voltage collapse scenario. A part of the system is able to recover its voltage when renewable power decreases. Figure 18 gives voltage response in the continuous low voltage scenario. The system can recover stably with a decreased renewable power, which equally means an increase of synchronous generator.

It is notable that some renewables demonstrate new

TABLE X
INTUITIVE EVALUATION AND INFLUENCING FACTOR IN MODEL TESTS

Model Name	Scenarios of the Model	Intuitive Evaluation	Influencing Factors
CSEE -VS (Voltage Stability)	Voltage Collapse	Time of Voltage Collapse	Renewable penetration, HVDC power level, configuration of synchronous condenser, load level, etc.
	Continuous Low Voltage	Steady Voltage Level	
CSEE -RAS (Rotor Angle Stability)	Dynamic (Periodic) RAS	Damping Ratio	Series compensation, thermal generation arrangement, inter-area power transmission, etc.
	Transient (Aperiodic) RAS	Critical Clearing Time	
CSEE -FS (Frequency Stability)	High Frequency	Frequency Zenith/Nadir, Time of the Zenith/Nadir, Steady Frequency Deviation	System inertia, HVDC power level, types of system fault (e.g., HVDC commutation failure, HVDC block out), load variation, etc.
	Low Frequency		
	Ultra-Low Frequency Oscillation	Frequency and Amplitude of Oscillation	
CSEE -PFO (Power Frequency Overvoltage)	Temporary PFO	Voltage Maximum and Voltage Rise	Configuration of converter station, contingency control strategy, renewable penetration, etc.
	Continuous PFO		

transient behaviors in the scenario of high penetration. As seen from the 1200MW curve in Fig. 16, the voltage oscillates abnormally during the time t=6s and t=7s. This is an LVRT-induced oscillation, which is rarely studied but reported in real power systems. The post-fault terminal voltage of renewables near the LVRT threshold (0.9p.u. in this model), making the renewable get in and out of LVRT control repeatedly. The LVRT control in turn affect the terminal voltage, and leads to voltage oscillation. To observe such phenomenon, active power output of one wind turbine in wind farm W1 is adopted and demonstrated in Fig. 19(a). Its terminal voltage is demonstrated in Fig. 19(b).

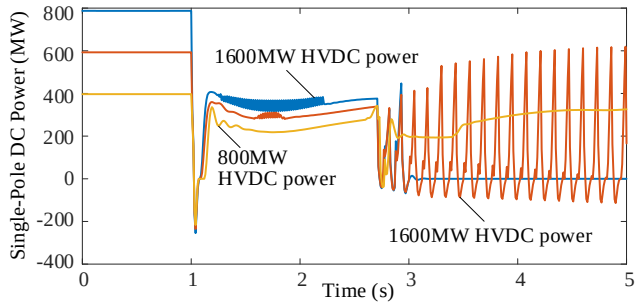

Fig. 15. HVDC response with varied DC power in voltage collapse scenario.

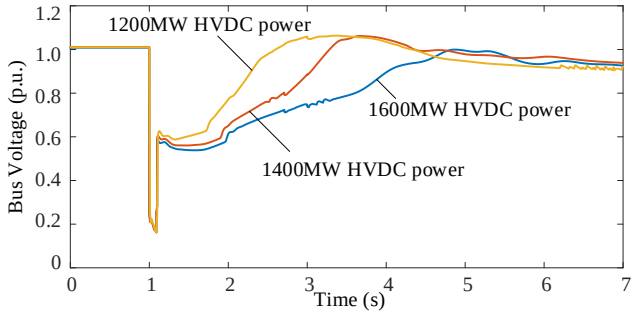

Fig. 16. AC voltage with varied DC power in continuous low voltage scenario.

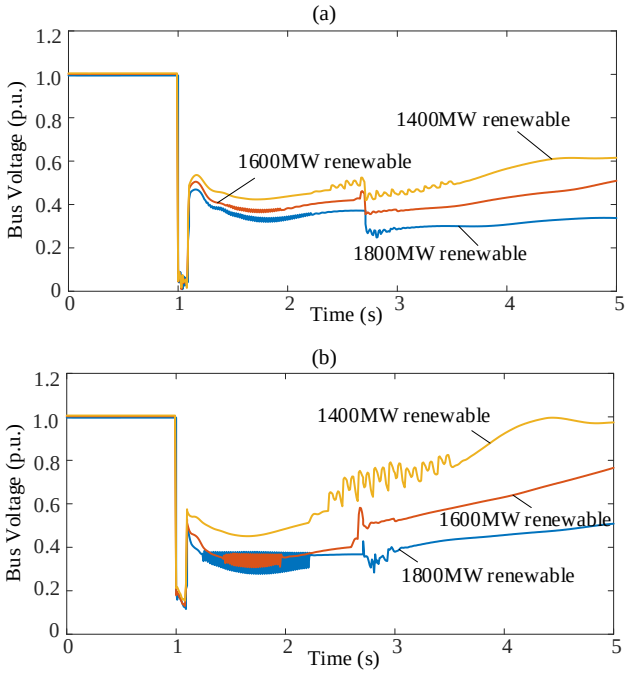

Fig. 17. Transient voltage of voltage collapse scenario with varied renewable power: a) voltage of bus_01, b) voltage of bus_05.

The results also highlight importance of the detailed renewable plant model in Fig. 1, as the LVRT control is highly dependent on the terminal voltage of renewables, rather than the PCC of renewable plant.

LVRT-induced renewable ramping and disconnection are not considered yet in the model. In real power systems, performance of the repeated LVRT can be more complex. This is dependent on renewable controls adopted by any users of the model.

B. Test of Rotor Angle Stability Model CSEE-RAS

In CSEE-RAS, the dynamic (periodic) RAS scenario is tested with varied series compensation, thermal generation arrangement, and renewable penetration. Tests of the former two factors are given in the main body of this paper, and the last is enclosed in the Supplementary Document of this paper.

In the test of series compensation, equivalent reactance of the critical transmission lines between bus_01 and bus_11 is

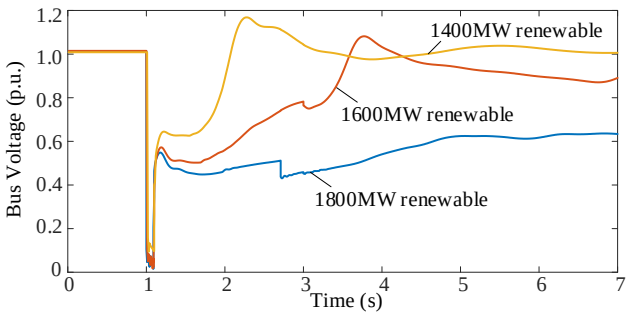

Fig. 18. Transient voltage of continuous low voltage scenario with varied renewable power.

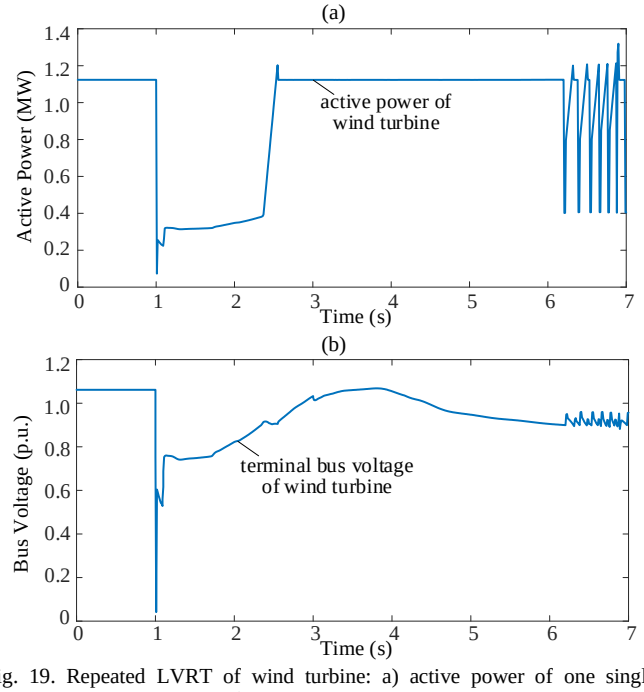

Fig. 19. Repeated LVRT of wind turbine: a) active power of one single turbine, b) terminal voltage of wind turbine.

adjusted. The line reactance and related system damping ratio is given in TABLE XI. The post-fault rotor angle oscillations between sending area and receiving area are demonstrated in Fig. 20 in time-domain. A lower series compensation results in a higher damping ratio, and benefits dynamic RAS.

In the test of thermal generation arrangement, three more scenarios are established in addition to the basic scenario. Thermal arrangement of all the four scenarios are listed in TABLE XII. Damping ratio of the scenarios are 0.0039, 0.0154, 0.0005, and 0.0116, respectively. The results have shown that an appropriate thermal arrangement helps to enhance dynamic RAS.

The transient (aperiodic) RAS scenario is tested with varied renewable penetration, inter-area AC power transmission, and thermal arrangement. Transient stability is evaluated by critical clearing time of the system, and is demonstrated in TABLE XIII-XIV and the Supplementary Document. The results have shown that transient RAS does not have distinct relation to overall renewable penetration of the system, but is related to the regional penetration in the sending/receiving end. In essence, it is related to the amount of inter-area power transmission.

Notably, rotor angle stability is closely related to controls or power devices. The controls are to be configured by the users. Only typical controls are applied in the test modes, which are adopted from practical engineering projects.

TABLE XI
DAMPING RATIO OF VARIED SERIES COMPENSATION

Line reactance (p.u.)	0.0126	0.0166	0.0206
Damping Ratio	0.0309	0.0039	0.0018

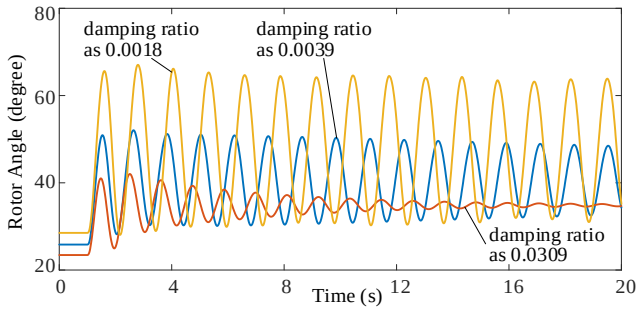

Fig. 20. Post-fault rotor angle oscillation with varied series compensation.

TABLE XII
VARIED THERMAL GENERATION ARRANGEMENT

Bus No.	Basic Scenario	Additional Scenario 1	Additional Scenario 2	Additional Scenario 3
03	400	794	/	400
04	400	400	400	400
05	/	/	/	/
06	396	/	801	399
09	480	480	480	240
10	300	300	300	300
11	300	300	300	540

C. Test of Frequency Stability Model CSEE-FS

In CSEE-FS, the high-frequency scenario is tested with varied HVDC fault, and varied renewable penetration. The former test is incorporated in the main body of this paper, and the latter is enclosed in the Supplementary Document.

The typical fault of HVDC is its block-out, whose impact has already been given earlier in Table VI. Another common HVDC fault is commutation failure (CF). In severe faults, CFs can occur successively for multiple times and in multiple HVDCs. TABLE XV evaluates frequency stability after different times of CF. In this table, CF occurs to all the three HVDCs, with an interval of 200ms. The results show that CFs increase frequency zenith, but do not create any steady frequency deviation. Related frequency dynamics are demonstrated in Fig. 21 in time-domain.

The low-frequency scenario of CSEE-FS is tested with varied load increasement. A sudden load increasement always decreases system frequency. Related system dynamics are shown in Fig. 22 in time-domain.

The ultra-low frequency oscillation is tested with varied inertia. Related results are given in Fig. 23, with quantifying

TABLE XIII
CRITICAL CLEARING TIME OF VARIED RENEWABLE PENETRATION

	Renewable in Sending Area (MW)	Renewable in Receiving Area (MW)	Renewable Penetration	CCT (s)
Basic Scenario	3890	1500	50.1%	0.156
Additional Scenario 4	4490	1500	55.6%	0.200
Additional Scenario 5	3290	1500	44.5%	0.131
Additional Scenario 6	3890	2100	55.7%	0.133
Additional Scenario 7	3890	900	44.5%	0.190

TABLE XIV
CRITICAL CLEARING TIME OF VARIED INTER-AREA AC TRANSMISSION

	Thermal Power (MW)	Renewable Power (MW)	Inter-Area AC Transmission (MW)	CCT (s)
Basic Scenario	5375	5390	3189	0.156
Additional Scenario 8	5100	5121	2877	0.180
Additional Scenario 9	5651	5660	3503	0.120

TABLE XV
FREQUENCY STABILITY EVALUATION OF VARIED HVDC CF

Times of CF	Frequency Zenith (Hz)	Time of the Zenith (s)	Steady Frequency Deviation (Hz)
2	0.51	1.40	0
3	0.71	1.59	0
4	0.87	1.69	0

indices given in TABLE XVI. Oscillating frequency is hardly affected by the system inertia and varied triggering fault, with only the former factor demonstrated here in the main body. Related simulation inertia. Amplitude of the oscillation increases along with the decrease of inertia.

D. Test of Power Frequency Overvoltage Model CSEE-PFO

In CSEE-PFO, the temporary PFO scenario is tested with varied system fault, varied renewable power, and varied HVDC power. The first of the test reveals a distinct PFO phenomenon induced by renewables, and is demonstrated in this section.

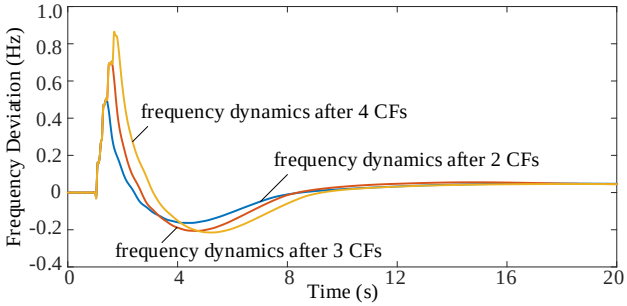

Fig. 21. Frequency dynamics after CFs.

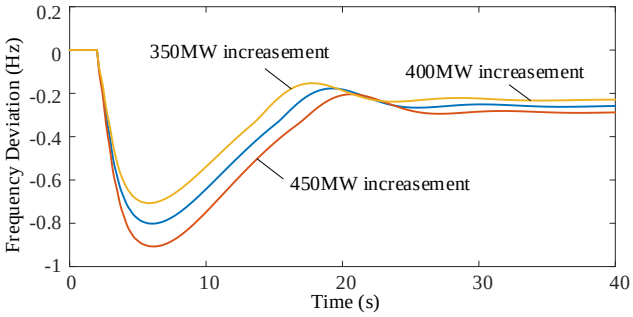

Fig. 22. Frequency response of the system with varied load increasement.

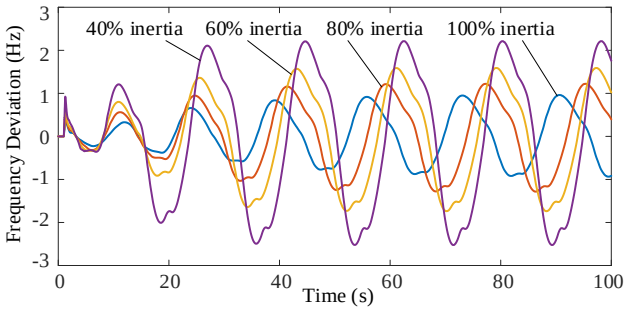

Fig. 23. Frequency response of the system with varied system inertia.

TABLE XVI
FREQUENCY OSCILLATION WITH VARIED INERTIA

System Inertia	Frequency of Oscillation	Amplitude of Oscillation
100%	0.056	1.61
80%	0.055	2.43
60%	0.055	3.06
40%	0.056	4.62

In this test, the HVDC fault is replaced by a three-phase-to-ground AC fault near wind turbine WT02-01, which disappears 0.1s later. Voltage dynamics of PCC of wind turbine and HVDC are demonstrated in Fig. 24. The maximum voltage is mainly induced by the time-delay of renewable LVRT. At the time of fault clearance, the system has recovered but LVRT control does not quit immediately. The renewable still create a significant amount of reactive power. This increases its terminal voltage. Occasionally, high-voltage-disconnection would occur to the renewable.

The continuous PFO scenario is tested with varied configuration of rectifier station, varied HVDC power level, and varied post-fault contingency control. All the results are enclosed in the Supplementary Document.

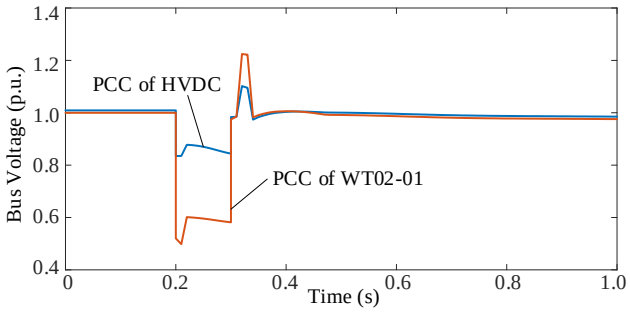

Fig. 24. Voltage dynamics after AC fault.

V. CONCLUSION

This paper presents a set of test models for stability/security study of modern AC-DC hybrid power systems with high penetration of renewables. All the models are extracted from real power systems, covering various aspects of voltage stability, rotor angle stability, frequency stability, and power frequency overvoltage in power systems. Renewable penetrations of the models are over 50%. Several renewable-induced distinct phenomena are incorporated, along with the conventional stability/security problems.

Performances of the models are tested in 27 different scenarios, with various influencing factors and disturbances. The results are presented either in the main body or the Supplementary Document of the paper, to serve as reference for all the users. All data can be accessed at https://github.com/lbl-hub/CSEE, along with related documents that describes details of the models. The data are in BPA format. For anyone who does not have BPA software, he/she can view the original data as .txt files. Besides, main data of the models are listed in tables in the document, aiding users who are not familiar with BPA.

When establishing the test systems, the previous versions have been used by several research institutes like Tsinghua University, and in several key R&D programs [27]-[29]. Some researchers have established the systems in other platforms like PSASP [30]. As electromagnetic simulation can better reflect dynamics of power electronic devices, some literatures also develop the test systems in electromagnetic platforms like DIgSILENT [31]. Having carefully considered all feedbacks from the researchers, the authors finally derived the test

systems in this paper. The CEPRI and CSEE herein heartily welcomes all further feedback from users of the models.

APPENDIX

A. Example of PV plant model

Figure A1 gives a PV plant model in the test system for power-frequency overvoltage, in which SC means synchronous condenser. Comparing the wind power plant in Fig. 1 and the PV plant in Fig. A1, the major difference lies in reactive compensation. The reason is that the PV plant is at the sending end of HVDC, and is constrained by overvoltage problems. Synchronous condenser provides a better dynamic voltage support.

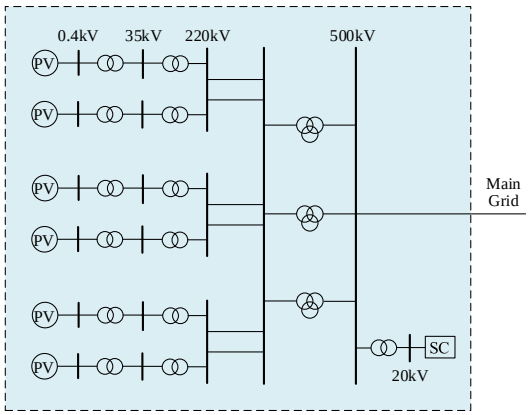

Fig. A1. Topology of a PV plant in CSEE-PFO.

B. Device-level dynamic model of renewables

Model of renewable sources in the test systems include type-III winds, type-IV winds, and PVs. Among the renewable sources, PV and type-IV wind have similar grid interface. The block diagram in Fig. A2 applies to both PV and wind. One can distinguish between PV and wind based on the generator model block in Fig. A2.

In the block diagram of Fig. A2, the active power control and reactive power control are very important in electromechanical simulations. Details of the controls are given in Fig. A3 and A4, respectively. One can refer to BPA manuals to obtain more details of the models.

Model of type-III wind is more complex, which is shown in Fig. A5. In type-III wind, reactive power of the turbine is controlled as zero. Reactive power of the grid-side converter is the same as what is shown in Fig. A4. Active power response of type-III wind is shown in Fig. A6.

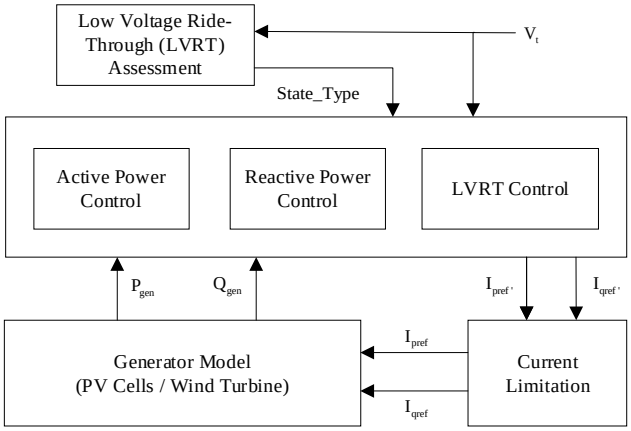

Fig. A2. Overall block diagram of PV and type-IV wind.

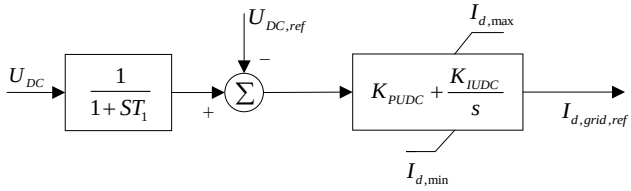

Fig. A3. Active power control of PV and type-IV wind.

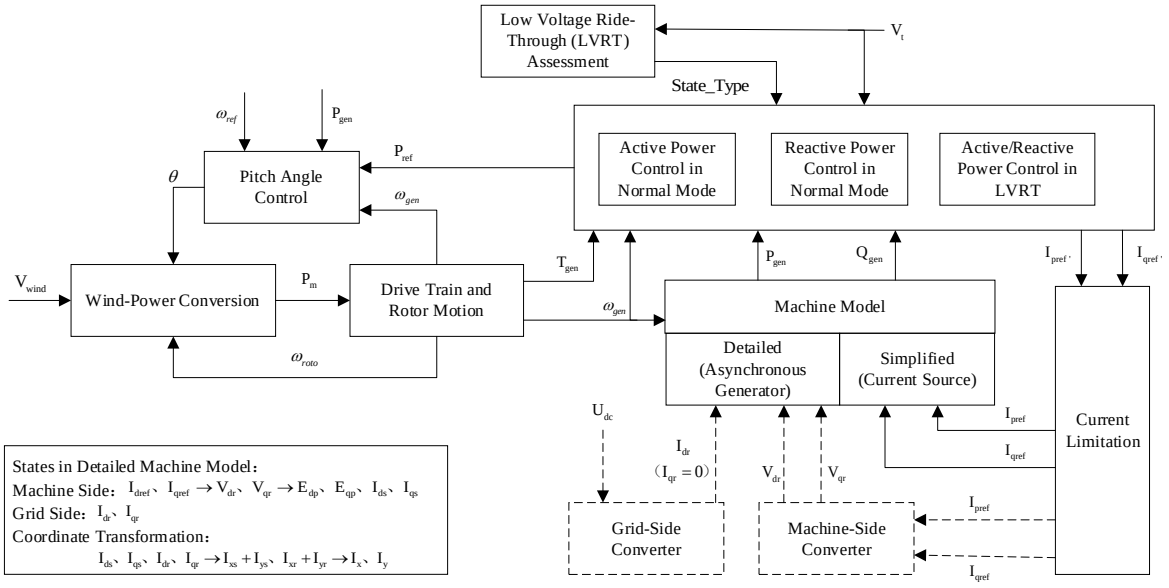

Fig. A5. Overall dynamic model of type-III wind.

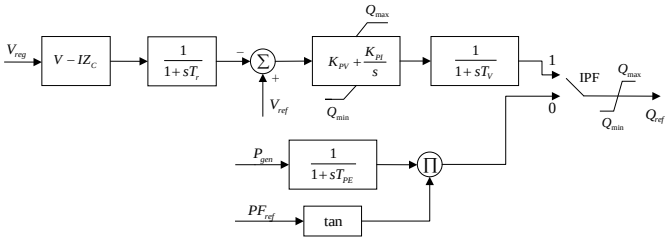

Fig. A4. Reactive power control of PV and type-IV wind.

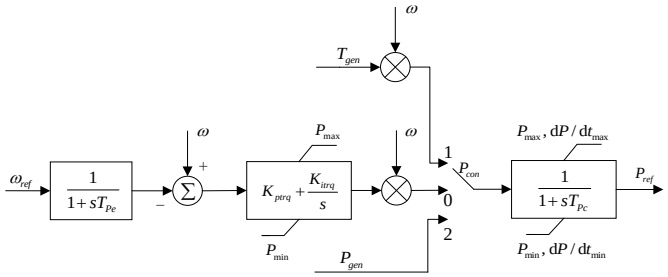

Fig. A6. Block diagram of the active power control of type-III wind.

The above models are electromechanical models in BPA. Similar models are adopted in other platforms like PSASP, and G. Cai *et al.* develop the test systems with more detailed electromagnetic models in DIgSILENT [31].

REFERENCES

[1] M. M. Hand et al., "Renewable electricity futures study. volume 1. exploration of high-penetration renewable electricity futures," National Renewable Energy Lab., Golden, CO, USA. [Online]. Available: https://www.nrel.gov/docs/fy12osti/52409-1.pdf

[2] National Development and Reform Commission, *China 2050 high renewable energy penetration scenario and roadmap study*, Energy Research Institute of National Development and Reform Commission, Beijing, China, Tech. Rep. EFCHINA-20150420, 2015. [Online]. Available: https://www.efchina.org/Reports-zh/china-2050-high-renewable-energy-penetration-scenario-and-roadmap-study-zh

[3] European Commission, *A European Green Deal*, [Online]. Available: https://commission.europa.eu/strategy-and-policy/priorities-2019-2024/european-green-deal_en

[4] N.Mithulananthan, "Hopf Bifurcation Control and Indices for Power System with Interacting Generator and FACTS Controllers", PhD dissertation, Department of Electrical and Computer Engineering, University of Waterloo, Canada, 2002.

[5] P. Kundur, N. J. Balu and M. G. Lauby, "Power system stability and control", McGraw-Hill New York, 1994.

[6] T. Athay, R. Podmore, and S. Virmani, "A practical method for the direct analysis of transient stability," *IEEE Trans. Power App. Syst.*, vol. PAS–98, no. 2, pp. 573–84, Mar. 1979.

[7] Richard D. Christie, *Power system test cases archive*, [Online]. Available: https://labs.ece.uw.edu/pstca/

[8] L. Sun and X. Zhao, "Modelling and Analysis of Frequency-Responsive Wind Turbine Involved in Power System Ultra-Low Frequency Oscillation," *IEEE Trans. Sust. Energy*, vol. 13, no. 2, pp. 844-855, April 2022.

[9] J. Seppänen, M. Lehtonen, M. Kuivaniemi and L. Haarla, "Long Term Characteristics of Ultra Low Frequency Oscillations in the Nordic Power System," in *2022 IEEE PES Innovative Smart Grid Technologies Conference Europe (ISGT-Europe)*, Novi Sad, Serbia, 2022, pp. 1-5.

[10] X. Jin and H. Nian, "Overvoltage Suppression Strategy for Sending AC Grid With High Penetration of Wind Power in the LCC-HVdc System Under Commutation Failure," *IEEE Trans. Power Electronics*, vol. 36, no. 9, pp. 10265-10277, Sept. 2021.

[11] C. Yin and F. Li, "Analytical Expression on Transient Overvoltage Peak Value of Converter Bus Caused by DC Faults," *IEEE Trans. on Power Syst.*, vol. 36, no. 3, pp. 2741-2744, May 2021.

[12] T. Lan, H. Sun, S. Xu, and B. Zhao, "Phenomena and mechanism of power system transient voltage stability dominated by low voltage ride-through of renewables," *Automation of Electric Power Systems*, early access.

[13] T. Lan, Y. Jing, S. Xu and B. Zhao, Modelling and Analysis of Abnormal Transient Performance in Bulk Power System Dominated by Low-Voltage-Ride-Through of Distributed Renewables, in *proc. of IET RPG*, Shanghai, China, 2023, pp.821-825.

[14] S. Wang, S. Xu, H. Sun and J. Bi, "Quantification method of maximum access capacity of renewable energy in multi-infeed system with temporary overvoltage constraints," *CSEE Journal of Power and Energy Systems*, early access.

[15] N. Hatziargyriou et al., "Definition and Classification of Power System Stability – Revisited & Extended," in *IEEE Trans. Power Syst.*, vol. 36, no. 4, pp. 3271-3281, July 2021.

[16] Y. Zhang, Y. Xu, Z. Y. Dong and P. Zhang, "Real-Time Assessment of Fault-Induced Delayed Voltage Recovery: A Probabilistic Self-Adaptive Data-Driven Method," *IEEE Trans. Smart Grid*, vol. 10, no. 3, pp. 2485-2494, May 2019.

[17] T. Lan, H. Sun, W. Zhong, Y. Jing, B. Zhao and J. Xu, "LCC-HVDC's Systematical Impact on Voltage Stability: Theoretical Analysis and a Practical Case Study," *IEEE Trans. Power Syst.*, vol. 38, no. 2, pp. 1663-1675, March 2023.

[18] "Calculation specification for power system security and stability GB/T 40581-2021," China, 2021. [Online]. Available: https://openstd.samr.gov.cn/bzgk/gb/newGbInfo?hcno=C1ECBFB7557D1E515707A57433A61C8D

[19] "Code on security and stability for power system GB 38755-2019," China, 2019. [Online]. Available: https://openstd.samr.gov.cn/bzgk/gb/newGbInfo?hcno=1D988D54A435E864E67CAA13217E8A99

[20] Y. Chen, S. M. Mazhari, C. Y. Chung, S. O. Faried and B. C. Pal, "Rotor Angle Stability Prediction of Power Systems With High Wind Power Penetration Using a Stability Index Vector," *IEEE Trans. Power Syst.*, vol. 35, no. 6, pp. 4632-4643, Nov. 2020.

[21] B. Wang, H. Sun, W. Li, C. Yang, et al. "Power system inertia estimation method based on maximum frequency deviation," *IET Renewable Power Generation*, 2022, 16(3): 622-633.

[22] IEEE Guide for Online Monitoring and Recording Systems for Transient Overvoltages in Electric Power Systems, IEEE Standard 1894-2015.

[23] T. Lan, H. Sun, Q. Wang and B. Zhao, "Synthesis Load Model With Renewable Energy Sources for Transient Stability Studies," *IEEE Trans. Power Syst.*, vol. 39, no. 1, pp. 1647-1663, Jan. 2024.

[24] Y. Jin, D. Wu, P. Ju, C. Rehtanz, F. Wu and X. Pan, "Modeling of Wind Speeds Inside a Wind Farm With Application to Wind Farm Aggregate Modeling Considering LVRT Characteristic," *IEEE Trans. Energy Conv.*, vol. 35, no. 1, pp. 508-519, March 2020.

[25] J. Li, H. Sun, W. Li, H. Wang, C. Tu, and J. Zhang, "Construction and Equivalence of Single-Machine Model of Renewable Energy for Large-Scale Power System Simulation," *CSEE Journal of Power and Energy Systems*, in press.

[26] Q. Shi, F. Li, and H. Cui, "Analytical Method to Aggregate Multi-Machine SFR Model with Applications in Power System Dynamic Studies," *IEEE Trans. Power Syst.*, vol. 33, no. 6, pp. 6355-6367, Nov. 2018.

[27] J. Liu, J. Liu, X. Liu, X. Liu and Y. Zhao, "Discriminative Signal Recognition for Transient Stability Assessment via Discrete Mutual Information Approximation and Eigen Decomposition of Laplacian Matrix," *IEEE Trans. Ind. Inform.*, early access.

[28] G. Cai, S. Zhou, C. Liu, Y. Zhang, S. Guo and Z. Cao, "Hierarchical under frequency load shedding scheme for inter-connected power systems," *Protection and Control of Modern Power Systems*, vol. 8, no. 2, pp. 1-12, April 2023

[29] B. Li, S. Xu, H. Sun, Z. Li and L. Yu, "System Strength Assessment Based on Multi-task Learning," *CSEE Journal of Power and Energy Systems*, vol. 10, no. 1, pp. 41-50, January 2024.

[30] G. Cai, S. Zhou, C. Jiang, and Z. Cao, "Online prediction and active control of regional transient frequency security of interconnected system based on model-data driven method," *Electric Power Systems Research*, vol. 226, 2024.

[31] G. Cai, L. Xuan, Z. Sun, and J. Chao et al., "Ambient data-based online identification and location of frequency oscillations," *International Journal of Electrical Power and Energy Systems*, vol. 157, 2024.